



POLİTEKNİK DERGİSİ

JOURNAL of POLYTECHNIC

ISSN: 1302-0900 (PRINT), ISSN: 2147-9429 (ONLINE)

URL: <http://dergipark.org.tr/politeknik>



A comparative investigation into the impact of shop-primer coating on weldability of S235JR steel using MAG and SAW processes

İmalat ön astar kaplamanın S235JR çeliğinin MAG ve SAW yöntemleriyle kaynaklanabilirliği üzerindeki etkisinin karşılaştırmalı olarak incelenmesi

Yazar(lar) (Author(s)): Cemil Çetinkaya¹, Ali Akay², Uğur Özdemir³

ORCID¹: 0000-0002-0298-1143

ORCID²: 0000-0001-7243-9395

ORCID³: 0000-0003-0521-4617

To cite to this article: Çetinkaya C., Akay A. and Özdemir U., “A comparative investigation into the impact of shop-primer coating on weldability of S235JR steel using MAG and SAW processes”, *Journal of Polytechnic*, 26(4): 1587-1600, (2023).

Bu makaleye şu şekilde atıfta bulunabilirsiniz: Çetinkaya C., Akay A. ve Özdemir U., “A comparative investigation into the impact of shop-primer coating on weldability of S235JR steel using MAG and SAW processes”, *Politeknik Dergisi*, 26(4): 1587-1600, (2023).

Erişim linki (To link to this article): <http://dergipark.org.tr/politeknik/archive>

DOI: 10.2339/politeknik.1323835

A Comparative Investigation into the Impact of Shop-Primer Coating on Weldability of S235JR Steel Using MAG and SAW Processes

Highlights

- ❖ Shop-primer coating of 75 μm and above thickness has adversely affected the weld performance and mechanical properties.
- ❖ No decrease in mechanical properties or difficulty in arc initiation was observed in welds made after 25 and 50 μm shop-primer coating
- ❖ The effects of shop-primer coating application on the SAW method are less significant compared to the MAG method (except at 75 μm coating thickness).

Graphical Abstract

The effect of the shop-primer coating of different thicknesses on the MAG and SAW welding performance of S235JR material was investigated.

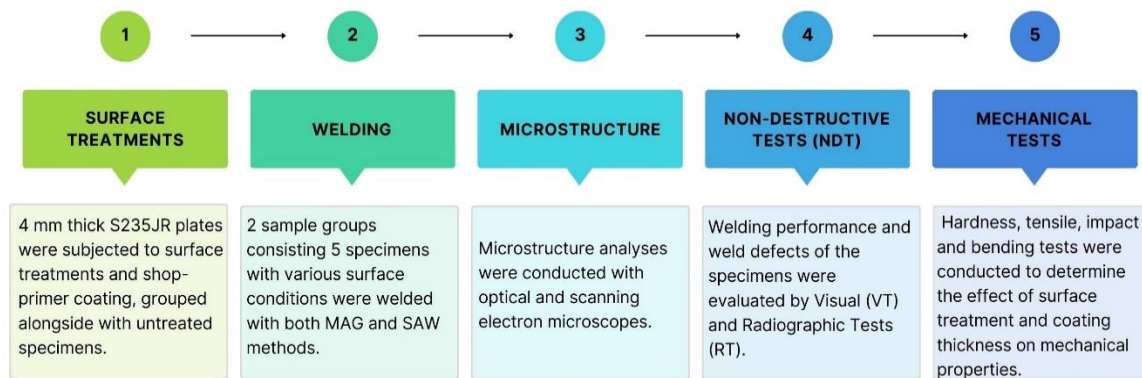


Figure. Schematic workflow of the study.

Aim

The aim of this study is to examine the effect of shop primer coating on weld quality and mechanical properties.

Design & Methodology

Samples different thicknesses of shop-primer coating, alongside with surface treated and as-received ones, were combined with 2 different welding methods (MAG and SAW), while parameters kept same for each welding method.

Originality

Weld quality, microstructure and mechanical properties were analyzed.

Findings

The shop primer coating did not have a negative effect neither to the weld performance, nor to the mechanical properties up to a certain thickness.

Conclusion

It has been observed that the thickness of the shop primer coating is the most important criteria for its weldability and arc initiation, and thick coatings reduce the mechanical properties and cause welding defects

Declaration of Ethical Standards

The Author(S) Of This Article Declare That The Materials And Methods Used In This Study Do Not Require Ethical Committee Permission And/Or Legal-Special Permission.

A Comparative Investigation into the Impact of Shop-Primer Coating on Weldability Of S235JR Steel Using MAG And SAW Processes

Araştırma Makalesi / Research Article

Cemil ÇETİNKAYA¹, Ali AKAY², Uğur ÖZDEMİR^{1*}

¹Gazi Üniversitesi, Faculty of Technology, Metallurgical and Materials Engineering Dpt, Ankara, Turkey

²Birikim Engineering Co., Ankara, Turkey

(Geliş/Received : 06.07.2023 ; Kabul/Accepted : 28.07.2023 ; Erken Görünüm/Early View : 04.09.2023)

ABSTRACT

The outcome of a welding process relies on various factors, one of which is the heat input at the welded joint. Consequently, the thermal conductivity of the plates to be welded holds significant importance, just like the selection of the welding technique. This research investigates the impact of applying Metal Active Gas (MAG) and Submerged Arc Welding (SAW) methods on differently coated (shop-primer) plates, as well as un-coated S235JR structural steel plates. The study explores how these applications, with varying heat inputs, affect the mechanical and microstructural properties of the materials. Filler metal of SG2/S2 non-alloy steel grade wires was employed. The variable parameters chosen included surface conditions, coating thickness, and heat input. It was observed that altering the coating thicknesses and welding methods led to welding defects. Non-destructive tests indicated that surface conditions and welding methods somewhat influenced the weld joint. Specimens with a thickness of 75 µm exhibited poor performance in tensile, impact, and bending tests. Fractography studies validated these findings.

Keywords: Sand blasting, surface coating, shop-primer, arc welding, microstructure.

İmalat Ön Astar Kaplamanın S235JR Çeliğinin MAG ve SAW Yöntemleriyle Kaynaklanabilirliği Üzerindeki Etkisinin Karşılaştırmalı Olarak İncelenmesi

ÖZ

Bir kaynak işleminin başarılı olması, kaynaklı bağlantıdaki ısı girdisinin de dahil olduğu birçok faktöre bağlıdır. Bu yüzden, kaynaklanacak plakaların ısı iletkenliği, kaynak yönteminin seçimi kadar önemlidir. Bu çalışmada, farklı kalınlıklarda imalat ön astar (shop-primer) ile kaplanmış ve kaplanmamış S235JR yapısal çelik levhalara Metal Aktif Gaz (MAG) ve Tozaltı Ark Kaynağı (SAW) yöntemleri uygulanmış ve bu uygulamaların değişen ısı girdileri ile malzemelerin mekanik ve mikroyapısal özellikleri üzerindeki etkileri araştırılmıştır. Alaşımız çelik kompozisyonundaki SG2/S2 telleri dolgu metali olarak kullanılmıştır. Değişken parametreler olarak yüzey koşulları, kaplama kalınlığı ve ısı girdisi seçilmiştir. Araştırma sonucunda değişen kaplama kalınlıklarının ve kaynak yöntemlerinin kaynakta hatalara neden olduğu gözlemlenmiştir. Tahribatsız testler, yüzey koşullarının ve kaynak yöntemlerinin kaynak bağlantısı üzerinde kısmen etkili olduğunu ortaya koymuştur. Çekme, darbe ve eğme testlerinde 75 µm kalınlığa sahip numuneler zayıf sonuç vermiştir. Sonuçlar fraktografi çalışmaları ile doğrulanmıştır.

Anahtar Kelimeler: Kumlama, yüzey kaplama, imalat ön astar, ark kaynağı, mikroyapı.

1. INTRODUCTION

For years, structural steels have continued to be the widely used structural material in the manufacturing industry, but the corrosion of these steels during fabrication is one of the main problem for all sectors. The application of diverse shop-primer coatings for corrosion protection during fabrication is extensively utilized worldwide. A solution using a variety of anti-corrosion protective fabrication pre-primer coatings is widely applied around the world. Arc welding is employed in various industries such as shipbuilding, bridge construction, power plants, and more, to fabricate steel

components. In these fabrications, the use of weldable shop-primer coating significantly speeds up and simplifies the preparation of structural members for assembly and welding. The shop-primer coating serves additional practical objectives, such as safeguarding structural components throughout the steel material production phase and providing protection during storage prior to the application of the initial paint system [1,2].

Typically, a shop primer is advised to have a film thickness ranging from 20 to 25 µm, a recommendation that is based on smooth test panels. None to low alloy steels coated with a shop primer can still be welded as needed [3]. In the research conducted by Blasko et al.,

*Sorumlu Yazar (Corresponding Author)
e-posta : uozdemir@gazi.edu.tr

they examined the weldability of shop-primer materials with a thickness of $20 \pm 2 \mu\text{m}$. Observations revealed that when robotically welding materials with a shop-primer coating, welding should be done with oscillation motions and welding speed should be kept slow. Interpass cleaning is not mandatory in multipass welding up to 3 layers [4]. T. Solic et al., in their study on the effects of shop-primer coating on weld joints, provided temporary protection by applying two-component epoxy shop-primer to the steel surface. The mechanical properties of the welds on the coated surfaces were tested, and it was stated that the shop-primer coating did not have a detrimental effect on the quality of the weldments [5]. However, it is thought that the defects such as pores and spatter in the welds made after shop-primer applications are caused by the coating. Conversely, the presence of a shop-primer coating decreases arc stability and contributes to elevated levels of spatter and porosity. These factors can potentially compromise the structural integrity, particularly when subjected to tensile stresses [6]. Some studies have been conducted to support the findings in this regard. D'Addona et al., in their study of laser removal of the shop-primer coating prior to welding of steel plates used in the shipbuilding industry, stated that the shop-primer layer would sublime at the high temperatures generated during the welding process and create porosity in the weld seam [7]. In their investigation of GMAW welding using the cold metal transfer method on zinc-coated steel, Ahsan et al. discussed the formation of weld pores resulting from heat input. [8]. It is stated that during the welding of shop-primer coated steel, the gases formed as a result of combustion may harm the health of the welder [9,10].

Another issue is that not all of the energy obtained during the welding process can be used to melt the base metal and filler metal, and a considerable amount of energy is lost during the welding process. Theoretically, the energy obtained in the welding process is spent to melt the welding wire and the workpiece. However, in practice,

energy is lost by spatter, conduction, metal vapor, and convection. Naturally, the amount of lost energy varies according to the welding method. The reasons for these energy losses are also related to the conditions under which the welding process is carried out [11]. Ertürk et al. has revealed important findings about the effects of different heat inputs, especially on the metallurgical and mechanical properties of the heat-affected zone, depending on the welding melting technique and the number of passes [12].

To investigate the impact of shop-primer coating on the welding ability of SAW and MAG processes at various welding efficiencies, experimental studies were conducted. The experimental study aimed to scientifically examine the effects of the shop-primer coating, followed by an evaluation of the obtained results.

2. MATERIAL and METHOD

This study utilized S235 JR structural steels, which are commonly favored in general construction. The chemical analysis of these steels is provided in Table 1, while the mechanical properties can be found in Table 2. The experimental studies employed sample sizes of $4 \times 150 \times 350$ mm for MAG welding and $4 \times 150 \times 500$ mm for SAW. Some of the samples underwent no surface treatment, while others were subjected to sandblasting, specifically Sa 2 ½ according to TS EN ISO 8501-1. This was done to eliminate any undesirable substances on the material's surface and enhance coating bonding. Subsequently, various thicknesses of the shop-primer coating were applied, as shown in Table 3. The MAG and SAW methods were employed to combine the samples after these procedures. After the welding, all samples underwent visual inspection, macro and microstructure analysis, radiography and mechanical tests. Figure 1 displays photographs of the sandblasting process.

Table 1. Chemical analysis of S235JR steel specimens (wt%).

C	Mn	P	S	Cu	Al	Cr	Ti	Fe
0.09	0.53	0.018	0.011	0.008	0.037	0.025	0.002	Rest

Table 2. Mechanical properties of S235JR steel.

Yield Strength (MPa)	Tensile Strength (MPa)	Elongation (%)
285	388	40

Table 3. Nomenclature and surface treatment status of the samples.

SAMPLE	WELDING METHOD	SURFACE TREATMENT	COATING THICKNESS
M1	MAG	No surface treatment	-
M2	MAG	Sandblasting	-
M3	MAG	Sandblasting + Shop-primer coating	$25 \mu\text{m} \pm 5$
M4	MAG	Sandblasting + Shop-primer coating	$50 \mu\text{m} \pm 5$
M5	MAG	Sandblasting + Shop-primer coating	$75 \mu\text{m} \pm 5$
T1	SAW	No surface treatment	-
T2	SAW	Sandblasting	-
T3	SAW	Sandblasting + Shop-primer coating	$25 \mu\text{m} \pm 5$
T4	SAW	Sandblasting + Shop-primer coating	$50 \mu\text{m} \pm 5$
T5	SAW	Sandblasting + Shop-primer coating	$75 \mu\text{m} \pm 5$

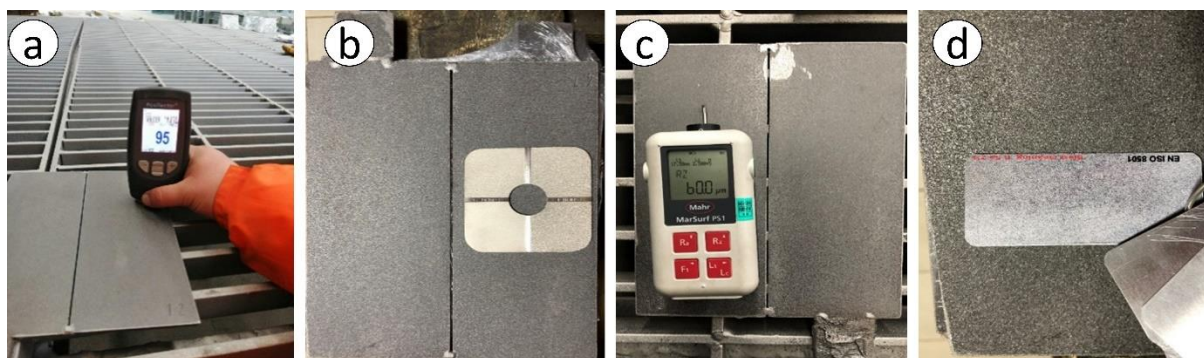


Figure 1. Sand-blasted sample photos, a) blasting measurement with needle tip gauge, b) blasting comparison plate, c) surface roughness measurement, d) blasting surface comparison photo.

Following sandblasting, the specimens received a shop-primer coating. This particular coating consists of an epoxy with two components; polyamide with zinc phosphate pigments, serving as effective anti-rust agent. Table 4 provides an overview of the main attributes of the coating employed in the investigations, while Table 5 presents its chemical composition. Additionally, Figure 2 depicts images of the samples after the application of the shop-primer coating.

Table 4. Properties of the shop-primer.

Color	Red
Solid matter ratio by volume	26 ± 1%
Hard Dry	6 min, 20°C
Method of Application	Air spraying
Max. thinner ratio by vol.	20%
Dry film thickness	20 µm ± 5



Figure 2. Photos of the samples after shop-primer application

Table 5. Typical shop-primer chemical composition (wt%)

H	P	Ca	Mg	Al	Cr	Zn	Si	O	C
5.8	1.5	5	3.3	0.2	0.8	3.8	3.2	35.6	43.8

Table 8. MAG and SAW parameters and consumables properties

Welding Method	Current (A)	Voltage (V)	Weld Speed (cm/min)	Wire Diameter (mm)	Gas Flow (l/min)	Heat Input (kJ/mm)
MAG	215-220	22	44	1.2	19-21	5.2
SAW	480-490	30	123	2.4	-	7.1

Table 6 provide details of the MAG and SAW wires utilized in welding all specimens, including those with shop-primer coating, along with their respective properties. Table 7 contains information about the SAW flux type and its properties. Additionally, Table 8 present the welding parameters that remained constant throughout the welding processes. M24 gas with 15% CO₂ and 2% O₂ addition in Argon was used as shielding gas in MAG welding.

Table 6. Welding wire properties used in MAG and SAW methods

TS EN ISO 14341-A: S2 Chemical Composition (wt%) - (Typical)			
C	Si	Mn	Cu
0.12	0.10	1.00	<0.30
Mechanical properties of filler metal			
Yield Str. (N/mm ²)	460		
Tensile Str. (N/mm ²)	525		
Elongation (%)	30		
Impact Toughness at -30 °C (J)	55		

Table 7. Welding flux properties used in SAW

TS EN ISO 14341-A SA AB 1 68 AC H5 AWS A5.17 F6A2-EL12 Chemical Composition (wt%) - (Typical)				
C	Si	Mn	Cu	Fe
0.07	0.35	1.50	-	Rest

3. RESULTS AND DISCUSSION

The primary goal of this study was to examine the alterations in the mechanical properties and phase transformations of S235JR materials following the application of MAG and SAW welding methods. Furthermore, the influence of surface preparation and varying shop-primer coating thicknesses on these welding techniques was examined. Visual inspections were performed on the samples individually, following the acceptance thresholds according to the TS EN ISO 5817 standard (B, C, and D criteria). Figures 3 and 4 illustrate visual representations of the cap and root seams of the parts welded using MAG and SAW methods, respectively.

Visual inspection was carried out by a certified controller according to Level 2 of the TS EN ISO 9712 standard.

The presence of weld defects such as insufficient penetration in the weld, the collapse of the root, and cracks was not observed in the other samples, except for the T5 sample, as a result of the visual inspection. However, due to the high current intensity and high welding speed, it was determined that partial undercut areas were formed in the samples, and these defects were within the limits of the acceptance criteria.

While welding of M3, M4, M5, T3, T4, and T5 specimens, a noteworthy correlation emerged where the emission of weld fumes exhibited an upward trend in tandem with the escalation of coating thickness. Additionally, upon meticulous examination of the post-welding rear surfaces of the coated specimens, a conspicuous intensification of black soot was observed, particularly in cases of higher coating



Figure 3. Photos of MAG welding cap and root passes.

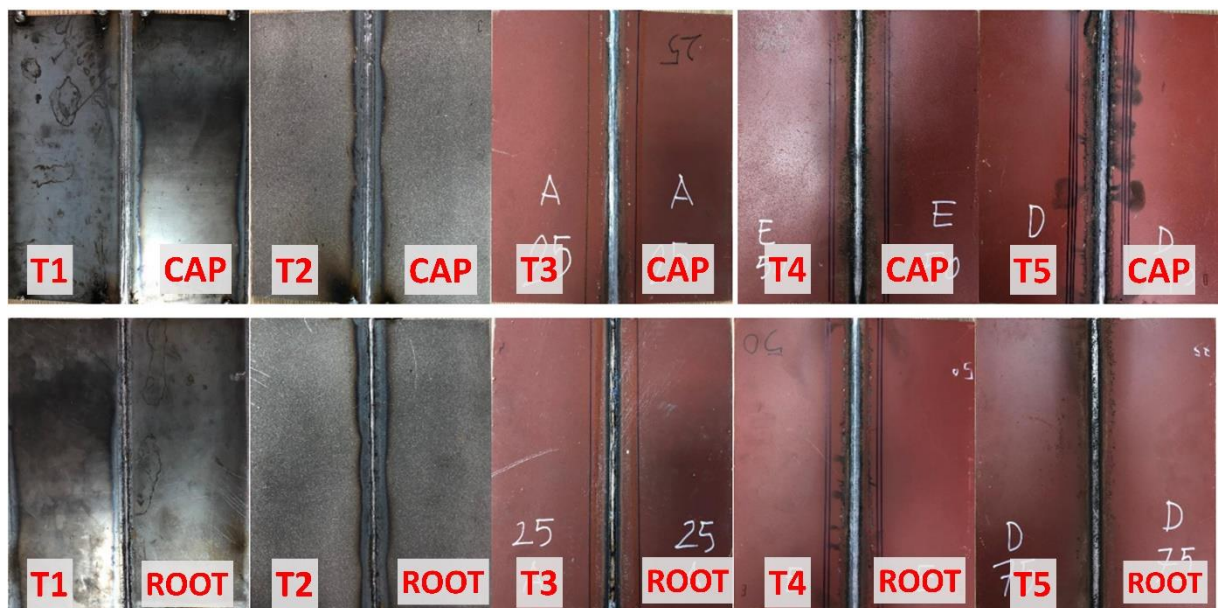


Figure 4. Photos of submerged arc welding cap and root passes.

thickness. In the literature, it has been stated that adequate ventilation should be provided during all welding processes of fabrication shop-primer-coated steels. Thus, the fume caused by the burnt coating will not have a harmful effect on the welding operator and the environment [13]. Among the samples welded with the SAW method, it was observed that penetration was not achieved, and sequential pores were formed only in the T5 sample. The samples welded using the MAG welding method exhibit an evident increase in black sooting as the coating thickness rises. According to the TS EN ISO 1090-2 standard, it is permissible to have primer paints on fusion surfaces, provided they do not pose any detrimental effects on the welding procedure. However, in the case of application grades EXC3 and EXC4, the presence of primers on fusing surfaces is restricted unless welding procedure tests adhering to EN ISO 15614-1 or EN ISO 15613 standards have been diligently conducted incorporating these primers [14].

Figures 5 and 6 display macrographs of samples welded using the MAG and SAW methods. Neither melting defects, nor lack of penetration (except T5), pores, cracks, and residues were detected in the samples during macrography examinations. The weld passes were wider and thicker in the SAW method compared to the MAG welding, due to higher heat input.

No excessive or insufficient penetration was observed in M3, M4, and M5 samples with a coating thickness of 25, 50, and 75 μm , and T3 and T4 samples with 25 and 50 μm . No effect of increasing the coating thickness on the weld penetration was observed in the specimens joined by MAG welding. This is because the gases released from the burnt shop-primer coating during welding are discharged from the weld pool with the help of shielding gas supplied at a high flow rate. In the research conducted by Solic et al., a meticulous investigation into the structural characteristics of S235JR steel subjected to MAG welding was undertaken. The authors reported that

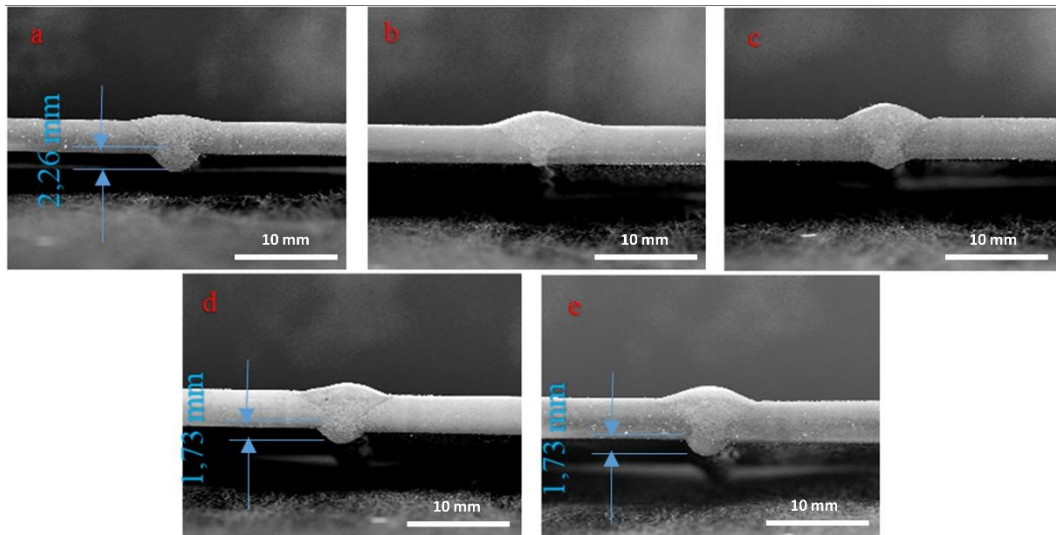


Figure 5. Macrographs of a) M1, b) M2, c) M3, d) M4, e) M5 specimens welded by robotic MAG welding method.

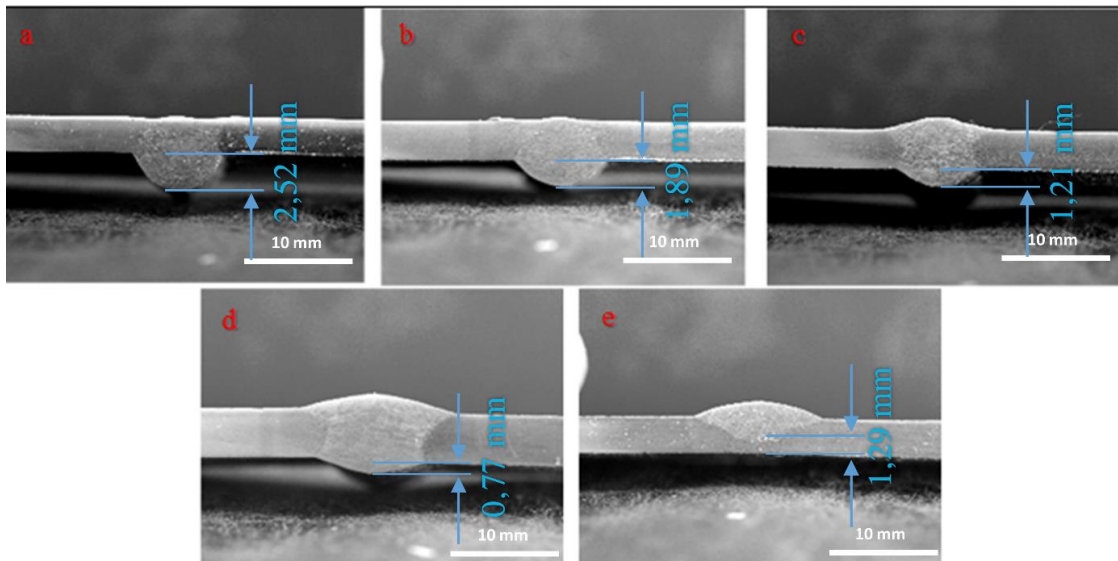


Figure 6. Macrographs of a) T1, b) T2, c) T3, d) T4, e) T5 specimens welded by SAW method.

the weld macrographs of samples coated with a protective layer exhibited a commendable absence of discernible defects or deviations, signifying the robustness and integrity of the welded joints [5].

It was observed that sufficient penetration was not achieved in the T5 sample, the thickest shop-primer coating with 75 μm . This is due to the fact that as the thickness of the shop-primer coating increases, the welding energy spent on burning the coating increases. Also, during welding, the organic binders used in the primer which burns during welding, break down to form hydrogen, water and carbon dioxide and hydrogen or water vapor, resulting in excessive spattering and, therefore, less deposited weld metal. In the specimens joined by SAW method, it is observed that as the coating thickness increases, excessive-penetration transitions to sufficient and eventually to insufficient penetration. It is seen that the amperage used in SAW is insufficient as the thickness increases due to increased combustion losses and spatter. As stated in Altınkök's study with MAG-TIG welds, the lack of penetration in the weld affects the strength of the weld seam. It has been reported that low penetration in the weld reduces the strength of the weld metal [15].

The microstructure of the S235JR structural steel is visually depicted in Figure 7, showcasing distinctive characteristics. Within the micrograph, the areas appearing lighter in color signify the existence of ferrite, while the darker regions correspond to the presence of the pearlite phase. This depiction provides valuable insights into the composition and arrangement of constituents within the steel matrix. The microstructure reveals a dominant presence of the ferrite phase and a relatively low ratio of the pearlite phase, which can be attributed to the low carbon content. Akkaş et al. explained that the microstructure of S235JR steel is composed of ferrite in the light-colored areas and a small number of perlite grains in the dark areas depending on the carbon content (0.09%) [16].

Micrographs of the specimens are given in Figures 8-17, respectively. The weld metal microstructures of the M and T group samples, which were welded using MAG and SAW methods respectively, exhibited the presence of the following structures; acicular ferrite (AF), Widmanstatten ferrite (WF), grain boundary ferrite (GBF), and polygonal ferrite (PF). Acicular ferrite, which

increases the strength and toughness of the weld metal, is formed by direct nucleation on inclusions in the interior of the austenite grains.

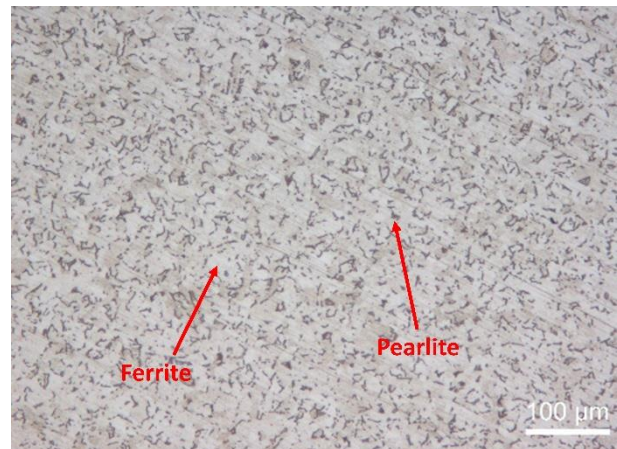


Figure 7. Microstructure of S235JR structural steel used in the study.

According to the literature, the interlocking structure due to the fine grain size of acicular ferrite provides maximum resistance to crack propagation by cleavage [17,18]. Polygonal ferrite occurring in austenite grains reduces the toughness due to its structure. Polygonal ferrite forms as coarse ferrite islands within previous austenite grains. Polygonal ferrite is similar to grain boundary ferrite and adversely affects toughness due to its coarse grain size [17]. Grain boundary ferrites are formed as a result of the austenite grains finding easier movement paths at their boundaries during cooling. In the literature, it has been explained that ferrite will form in the austenitic grain boundary since the austenitic grain boundary has an easier diffusion path [17]. Widmanstatten formed at the austenite grain boundaries grows into the ferrite grain and causes the strength of the weld metal to decrease. Widmanstatten ferrite is formed as a result of faster cooling than grain boundary ferrite in the temperature range of 750-650 $^{\circ}\text{C}$ [18].



Figure 8. Microstructure images of the M1 sample, a) weld metal, b) melting boundary, c) coarse-grained zone.



Figure 9. Microstructure images of the M2 sample, a) weld metal, b) melting boundary, c) coarse-grained zone.



Figure 10. Microstructure images of the M3 sample, a) weld metal, b) melting boundary, c) coarse-grained zone



Figure 11. Microstructure images of the M4 sample, a) weld metal, b) melting boundary, c) coarse-grained zone



Figure 12. Microstructure images of the M5 sample, a) weld metal, b) melting boundary, c) coarse-grained zone

Grains of the samples welded with the SAW method were found larger in the weld metal. Durgutlu et al. explained the reason for this differentiation with the high heat input in the SAW method [19]. It was observed that coarse-grained regions containing ferrite and pearlite are

formed in the melting boundary zones and HAZ of the M and T group samples as a natural result of the welding process.



Figure 13. Microstructure images of the T1 sample, a) weld metal, b) melting boundary, c) coarse-grained zone.

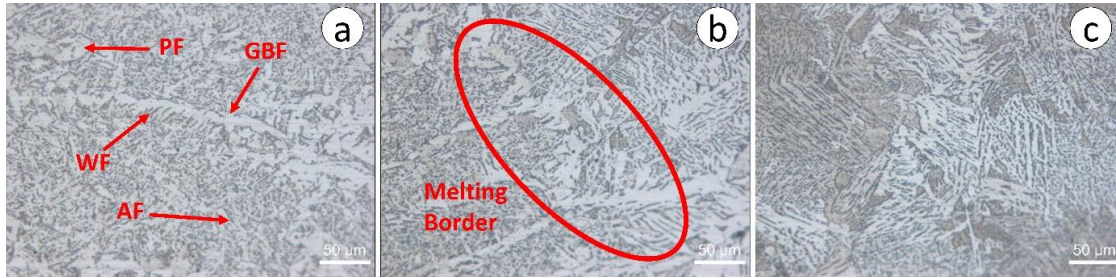


Figure 14. Microstructure images of the T2 sample, a) weld metal, b) melting boundary, c) coarse-grained zone.

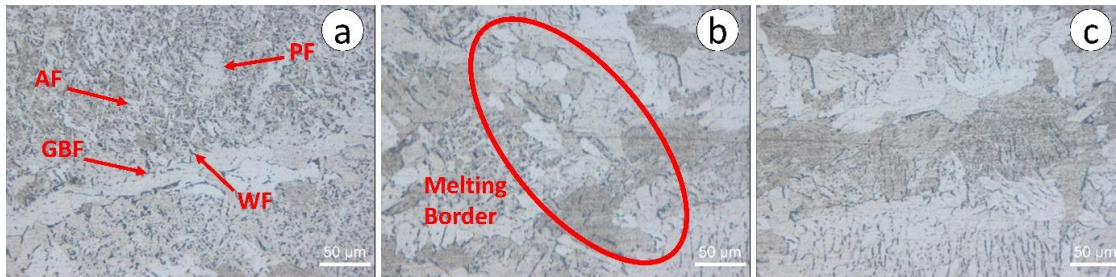


Figure 15. Microstructure images of the T3 sample, a) weld metal, b) melting boundary, c) coarse-grained zone.



Figure 16. Microstructure images of the T4 sample, a) weld metal, b) melting boundary, c) coarse-grained zone.



Figure 17. Microstructure images of the T5 sample, a) weld metal, b) melting boundary, c) coarse-grained zone.

Microstructure investigations conducted on both coated and uncoated samples joined by MAG and SAW revealed that, except for the T5 sample, the shop-primer coating had an insignificant impact on the microstructure. It is understandable to have differences in grain structure and size as a result of different heat inputs due to different welding methods. Sandblasting did not result in any discernible positive or negative effects on the microstructures of the M2 and T2 samples. Nonetheless, within the subset of M3, M4, M5, T3, T4, and T5 samples, featuring a range of shop-primer thicknesses at 25, 50, and 75 μm , it was only in the case of the T5 sample that discernible influences stemming from the coating thickness were detected. In the coarse-grained region of the T5 sample, the grains were smaller than in the other samples. It was detected that the HAZ width

was much narrower than the other samples due to the low heat input. According to Çetinkaya et al., the hindrance in heat flow can be attributed to the excessive thickness of the shop primer coating [20]. Figures 18 and 19 depict radiography images showcasing the weld zones of the M and T grouped samples, respectively, which were joined using MAG and SAW methods.

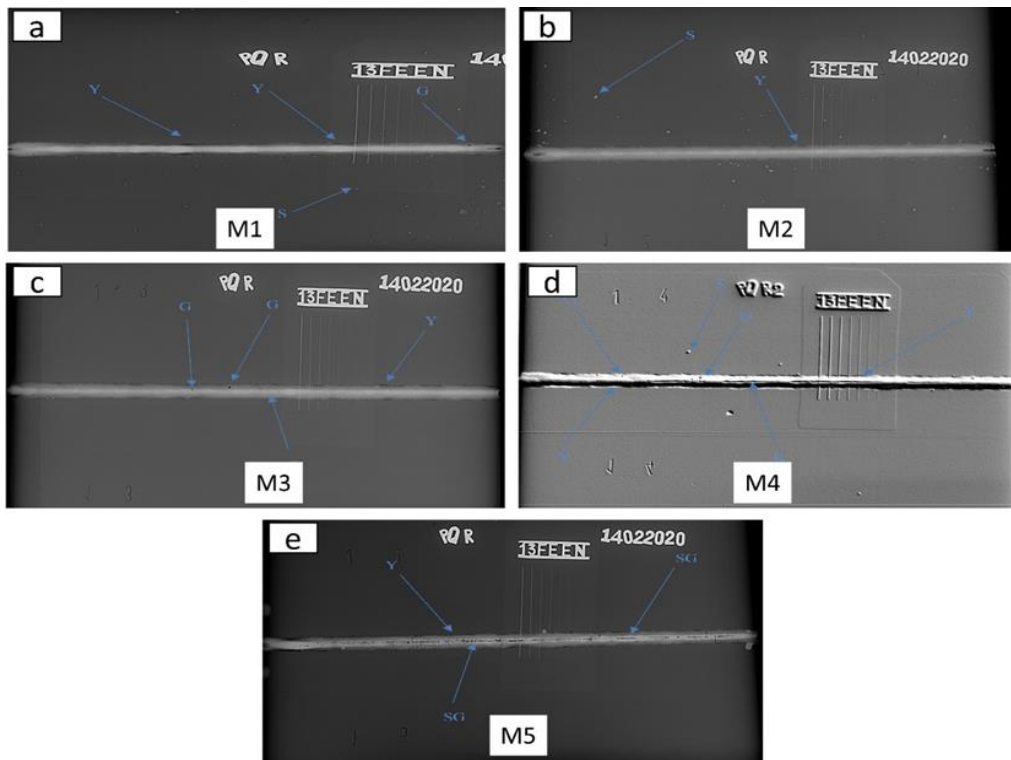


Figure 18. Radiography photographs of the weld area of the specimens welded by the robotic MAG a) M1, b) M2, c) M3, d) M4 and e) M5 [1].

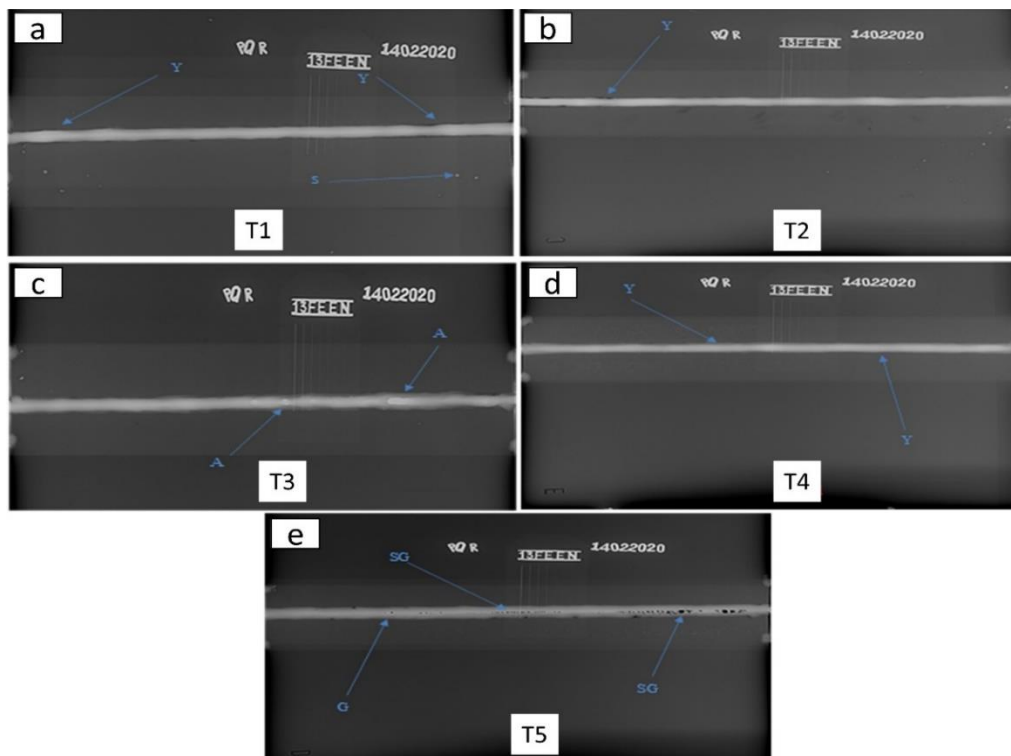


Figure 19. Radiography photographs of the weld area of the specimens welded by SAW a) T1, b) T2, c) T3, d) T4, and e) T5 [20].

In the radiography photographs of M1-5 and T1-5 samples given in Figures 18 and 19, undercut (Y), pore (G), spatter (S), excessive penetration (A), and sequential

pore (SG) have been detected, and these defects are within the TS EN ISO 10675-1 evaluation thresholds, except for M5 and T5. The pore and sequential pores in

the samples meet the requirement of a maximum 3 mm width specified in the acceptance criteria. In a study by Blasko et al. with portable welding robots, it was reported that the inorganic Zn surfacing thickness, has a slight influence on the weldment if the welding parameters (especially the welding speed) and the selection of appropriate welding consumables are properly controlled [4]. The pores detected in the M3 and M4 samples, and the pores in the M5 and T5 samples which are outside the acceptance criteria, are thought to be formed as a consequence of the burning of the coating. In the study on the welding of shop-primer coated Weldox and Hardox steels, it was stated that the pore formation would be minimized by removing the coating before welding, and it was observed that the pore formation increased to some extent in the welds made without removing the coating. Moreover, it has been noted that flux-cored MAG welding and MMA welding form fewer pores than other welding methods [13].

Figure 20 shows the indentation spots on the specimens where the hardness measurements are taken and Figure presents the hardness values of the samples welded using MAG and SAW techniques. In the Figure 20, (0) signifies the weld metal, (1) and (-1) represent HAZ, and (2) and (-2) represent the unaffected parent metal.

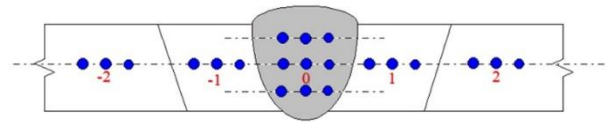


Figure 20. Illustration of the hardness indentation spots of the specimens.

According to the graph given in Figure 21, the hardness values obtained in all samples are obtained in the highest weld metal, then in the HAZ. Due to the limited carbon content (less than approximately 0.2%) in the base metal of plain carbon steel, the formation of martensite in the heat-affected zone (HAZ) during welding is not possible. Therefore, in the region close to the melting zone, the metal will come out at very high temperatures, and coarse grains will form. After cooling, a region with relatively low hardness and strength emerged. The elevated carbon content present in the filler metal accounts for the notable hardness augmentation observed within the weld zone. According to the study conducted by Demirbaş and Apay, the hardness increase observed in the weld metal is influenced by the chemical composition of the filler metal [21]. In M5 and T5 samples with high coating thicknesses, hardness values lost their homogeneity and linearity, especially in the HAZ. No significant hardness difference was observed in welded specimens with low-thickness coatings. Three tensile tests were performed on all samples welded with MAG and SAW, and the mean tensile test results are given in Table 9.

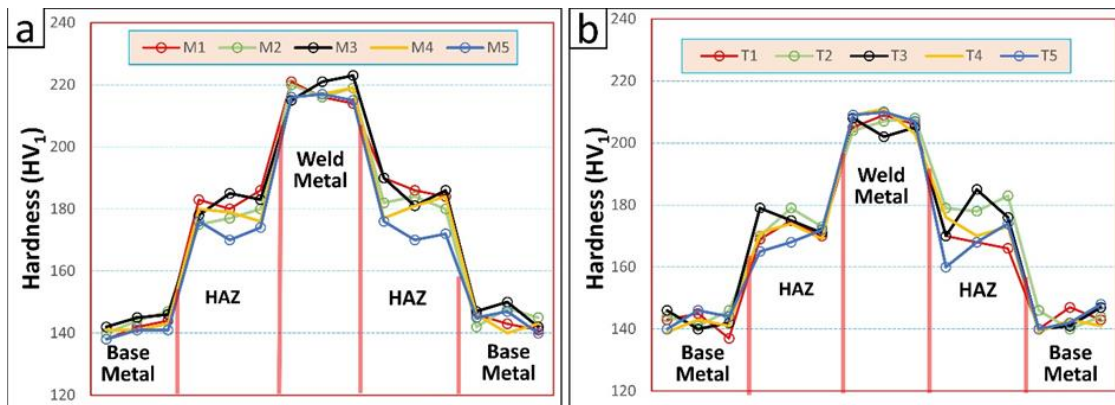


Figure 21. Hardness graph of the samples, a) M group, b) T group [1,20].

Table 9. Average tensile test results of the samples.

Sample No.	Crosshead Speed (mm/min.)	Tensile Str. (MPa)	Cross-sectional Narrowing (%)	Elongation (%)
M1	15	402	55	25.5
M2		403	58	24.1
M3		401	56	24.4
M4		402	57	24.5
M5		400	57	23.5
T1	15	403	57	22.2
T2		401	58	22.5
T3		397	57	22.8
T4		403	58	22.7
T5		256	10	1.4

The SEM images depicted in Figure 22 capture the fracture surfaces of the samples following the tensile test. Ductile fracture characteristics were evident in the fractographs of all specimens, even those displaying lack of penetration.

metal, even with lower carbon and/or alloy content in the weld deposit [22-23]. No significant effect of shop-primer coating on tensile and yield strengths and elongation was observed, except for specimen T5, which had a high coating thickness with a lack of penetration

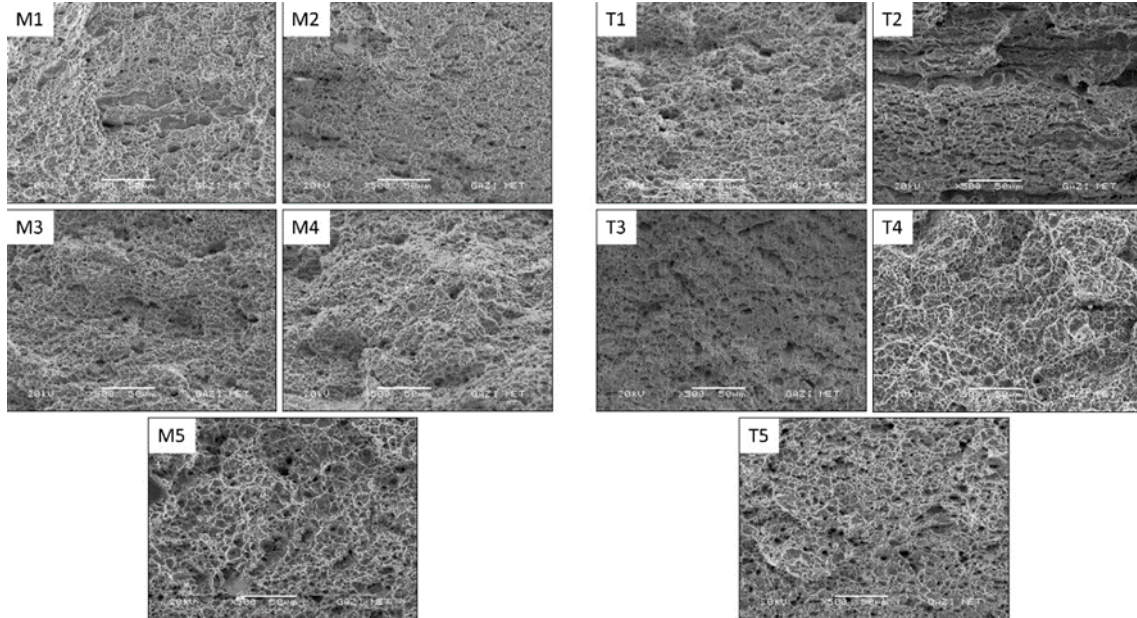


Figure 22. SEM images of the fractured surfaces of the specimens.

With the exception of the T5 sample, which fractured in the tensile test at the weld metal, all other samples experienced a rupture in the base metal. An increase in tensile strength on a small scale was observed in the welded samples in comparison to the base metal. This increase in strength was attributed to the enhanced strength in the HAZ and weld metal resulting from the welding process, leading to greater force requirements for deformation in these regions. Previous studies have demonstrated that the weld metal typically contains a relatively high concentration of dislocations, which contributes to the elevation of yield strength in C and C-Mn steels. Consequently, the weld metal exhibits higher tensile and yield strength compared to the equivalent base

and high porosity.

The fractograph of S235JR steel displayed characteristics of ductile fracture, which can be attributed to its structure and low carbon content. Previous studies have also mentioned that fracture can arise from the coalescence of voids or mechanical instability within the material itself. Initially, pits form in inclusions and subsequently expand through plasticity. When these voids intersect, a crack emerges, leading to material failure. Ductile fracture commonly occurs in S235JR and similar materials that undergo plastic deformation [24-26].

The graph in Figure 23 illustrates the results of the notch impact tests conducted on the samples joined using MAG and SAW methods.

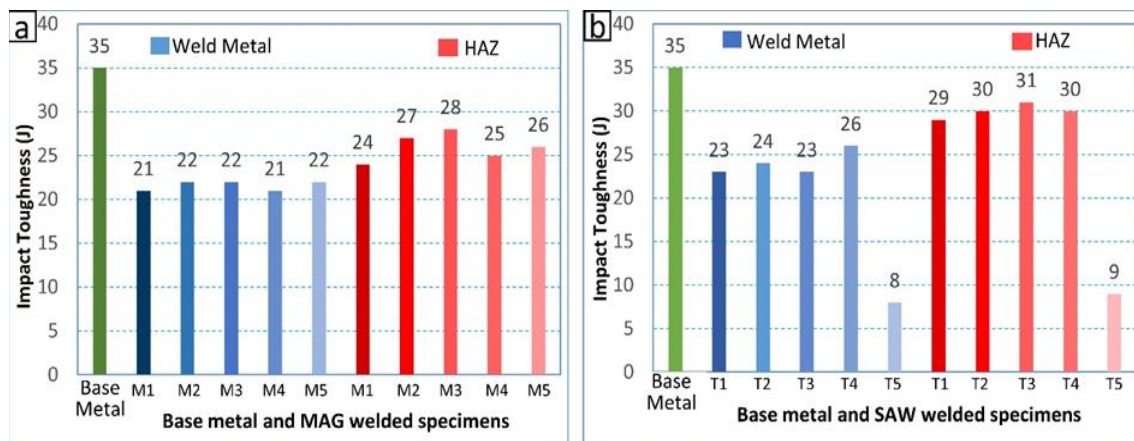


Figure 23. Notch impact results of a) M and b) T sample groups [1,20].

As anticipated, a reduction in toughness was observed in the samples from the M and T groups, which were welded using MAG and SAW methods, compared to the base material. This decline in toughness was evident in all notch impact tests performed on both the weld metal and HAZ. In the T group samples, the notch impact strength was slightly higher, which could be attributed to variations in heat input and cooling rates. The T5 samples with the thickest coating exhibited the lowest impact absorption value due to inadequate weld penetration. A captivating trend emerged in the notch impact values of the samples, showcasing the base metal with the highest values, followed by the HAZ, and finally the weld metal exhibiting the lowest values. This decline in toughness within the weld metal can be attributed to the interplay of factors such as the composition of the filler metal and the cooling regime employed during the welding process. Coatings of thicknesses that did not cause lack of penetration and high porosity in the weld had no effect

compressive stress. If the material undergoes deformation within its elastic limit under the applied load, it indicates a ductile structure [29-31]. No failure or cracks were detected in the bending tests of the M1-4 and T1-4 samples, and the welds of the samples were considered to be successful. The formability of butt joints is satisfactory according to the bending test result.

As a result of the bending test and conformity assessment of the welds of the welded samples by applying different surface treatments, it was determined that all joints gave successful results, except for the M5 and T5 samples. No negative effect of shop-primer coating below 75 µm was found in the bending test. In the study of Solic et al., they reported that there was no negative influence in the bending tests of 15 µm thick shop-primer coated weldments, in other words, no visible mechanical damage was detected on the weld face or the weld root after being exposed to bending [5].

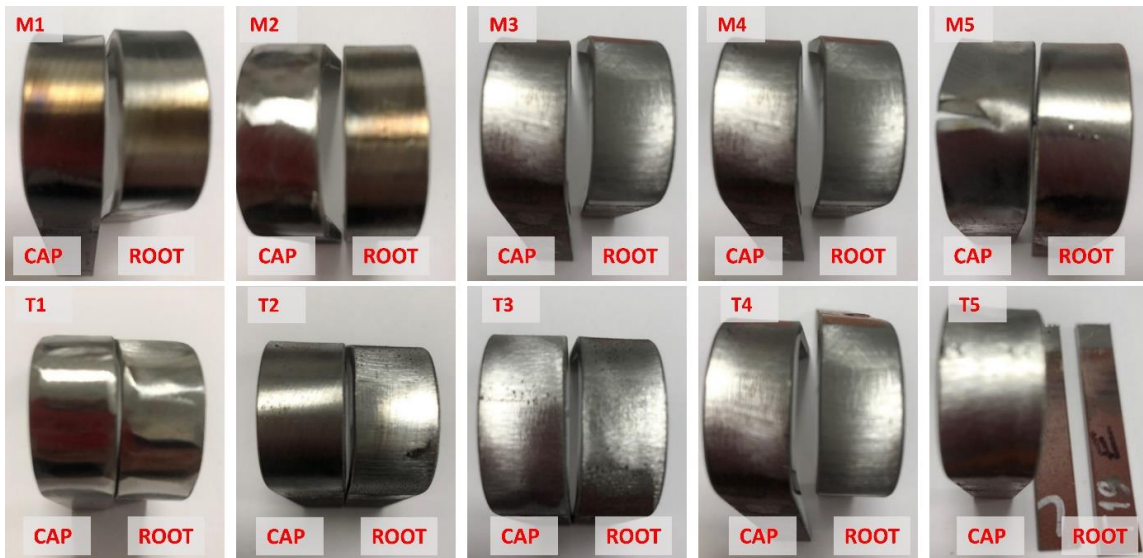


Figure 24. Images of specimens after bending test.

on impact toughness. However, both the weld metal and HAZ of the T5 specimen with insufficient penetration exhibited relatively low toughness.

On the other hand, in the HAZ, increased hardness resulting from grain coarsening and the cooling rate led to lower impact energy absorption compared to the base metal. In a study conducted by Durgutlu et al., it was found that weld metal has the lowest impact toughness while base metal resulted in highest values [27]. Another study by Çetinkaya reported a decrease in toughness as hardness increased, with the weld metal exhibiting lower notch impact strengths compared to the HAZ [28].

In Figure 24, the cap and root bending test result picture of the samples joined with MAG and SAW methods is given. The bending test involves subjecting a metal to plastic deformation along a linear axis, while the surface area remains relatively unchanged. This process induces tensile stress on one side of the specimen outside the neutral axis, while the other side experiences

6. CONCLUSION

In this study, S235JR grade steel plates with 4 mm thickness were initially divided into two groups; one group was welded using MAG method and the other group with SAW method with or without surface treatment. The following conclusions were drawn from this comparative study:

- It was observed that starting the arc became more difficult due to the increasing coating thickness, and the amount of generated fume during welding increased.
- Except for the sample with the highest coating thickness (T5) joined with the SAW method, no defects such as low or excess welding cap, which are welding surface defects, and collapsed root were not found in the other M and T group samples as a result of visual inspections. It was concluded that the lack of full penetration in the T5 sample was due to the high coating thickness.

- Except for the T5 sample, it was seen that the weld penetration was appropriate for all specimens, welding defects were not encountered, but the heat input affected the HAZ width. Full penetration could not be obtained in the T5 sample with the highest coating thickness. Therefore, the coating thickness affected the macrostructure examination results.
- The macrographs revealed the formation of similar microstructures in the samples joined using both MAG and SAW methods. The weld metal microstructures were identified to consist of GBF, WF, AF, and PF. The microstructure remained unaffected by variations in coating thickness and surface preparation. However, it was noticed that the grain structure in the coarse-grained area of the samples joined using the SAW method exhibited a larger size.
- The hardness values of the samples exhibited a gradual decrease from the weld metal to the unaffected base metal, and the hardness values were slightly higher in robotic MAG welding compared to SAW welding. No correlation was found between hardness results and coating thickness. However, especially in HAZ, nonlinearity observed in hardness results in specimens with 75 µm coating thickness.
- Shop-primer coatings up to 75 µm did not effect the post-weld mechanical properties (tensile strength, impact toughness, bending strength) drastically. Specimens with 75 µm thick coatings, however, showed less than satisfactory mechanical properties due to a lack of penetration and porosity formation.
- The effects of shop-primer coating application on the SAW method are less significant compared to the MAG method.

DECLARATION OF ETHICAL STANDARDS

The authors of this article declare that the materials and methods used in this study do not require ethical committee permission and/or legal-special permission.

AUTHORS' CONTRIBUTIONS

Cemil ÇETİNKAYA: Performed the experiments and analyzed the results.

Ali AKAY: Performed the experiments and analyzed the results.

Uğur ÖZDEMİR: Methodology and review & editing.

CONFLICT OF INTEREST

There is no conflict of interest in this study.

KAYNAKLAR (REFERENCES)

- [1] Çetinkaya C., Akay A., Arabacı U., and Özdemir U., "Effect of shop-primer coating on S235JR steel on MAG weldability", *Advances in Materials Science*, 22(2): 49-63, (2022).
- [2] Zhabrev L., Dmitry K., Igor M., and Oleg P., "The Coatings Breakdown Products Influence on the Gas Metal Arc Welding Parameters", *Coatings*, 10(11): 1061, (2020).
- [3] Hempel, "How to select the right paint system - Guidelines for corrosion protection in accordance with ISO 12944", Available: <https://www.hempel.com> (accessed on 11 June 2023).
- [4] Blasko G. J., Moniak D. J., and Howser B. C., "Evaluation of Hitachi Zosen Portable Welding Robotics", *SP-7 Welding Panel, The National Shipbuilding Research Program*, Wisconsin, 3-5, (1992).
- [5] Solic T., Maric D., Jagodic Z., Samardzic I., "Testing of the Shopprimer's Influence on the Quality of Welded Joint" *Metallurgija*, 56(3-4): 357-360, (2017).
- [6] Hong S. and Lee J., "Effects of hybrid welding parameters on porosity formation in C-Mn steel for shipbuilding", *24th International Congress on Laser Materials Processing and Laser Microfabrication*, Miami, 554-559, (2005).
- [7] D'Addona D. M., Genna S., Giordano A., Leone C., Matarazzo D., and Nele L., "Laser Ablation of Primer During the Welding Process of Iron Plate for Shipbuilding Industry", *9th CIRP Conference on Intelligent Computation in Manufacturing Engineering*, Naples, 464-469, (2014).
- [8] Ahsan Md. R. U., Kim Y. R., Ashiri R., Cho Y. J., Jeong C., and Park Y. D., "Cold Metal Transfer (CMT) GMAW of Zinc-Coated Steel". *Welding Journal*, 95: 120-132, (2016).
- [9] Volpone M. and Mueller S., "Problems linked to welding and cutting of primer treated metal sheets", *Welding International*, 20(12): 942-947, (2006).
- [10] Rexach A., Naik S. and Taylor A., "Weldable Anticorrosion Coatings for Steel Protection", *European Corrosion Congress*, Montpellier, 2578, (2016).
- [11] Kongel A., "Ergitme esaslı kaynak uygulamalarında kimyasal bileşimi etkileyen faktörlerin incelenmesi", *MSc Thesis*, Yıldız Technical University Institute of Science and Technology, (2005).
- [12] Ertürk İ., Durukan T., and Şentürk B., "Çeliklerin Kaynağında Isıdan Etkilenen Bölgenin Mikro Yapı Ve Özelliklerinin Tahmini", *10th Welding technology national congress and fair*, Ankara, 337, (2017).
- [13] SSAB, "A Guide to Better Welding of Hardox and Strenx - Welding Handbook", 2nd Edition, Available: www.ssab.com (accessed on 17 June 2023).
- [14] EN 1090-2, "Execution of steel structures and aluminum structures - Part 2: Technical requirements for steel structures", (2018).
- [15] Altınkök N., "MAG-TIG-Tozaltı Kaynak Bağlantısının Sonlu Elemanlar Yöntemi ile Termal Analizi", *Karaelmas Science and Engineering J.*, 7: 536-544, (2017).
- [16] Akkaş N., Onar V., and Varol F., "Raylı Sistem Araçlarında Kullanılan S235JR(Cu) Çelik Sacların Direnç Nokta Kaynağında Mikro Yapı Analizi", *3rd International congress on vocational & technical sciences*, Gaziantep, 1591-1599, (2018)

- [17] Parmar, R.S., “Welding Engineering and Technology”, (First Edition), *Khanna Publisher*, India, 659-700, (1995).
- [18] Ghandi A., Shamanian M., Salmani M. R., and Kangazian J., “Improvement of the microstructural features and mechanical properties of advanced high-strength steel DP590 welds”. *Int. J. Miner. Metall. Mater.*, 28: 1022–1029, (2021).
- [19] Durgutlu A., Gülenç B. and Tülbentci K., “Ark Kaynağında Kaynak Hızının Nüfuziyete ve Mikroyapıya Etkisi”, *Tr. J. of Engineering and Environmental Science*, 23: 251-259, (1999).
- [20] Çetinkaya C., Akay A., Arabacı U. and Fındık T., “S235JR malzemeye uygulanan astar kaplamanın tozaltı ark kaynak kabiliyetine etkisi”, *Journal of Polytechnic*, 25(3): 1335-1348, (2022).
- [21] Apay S. and Demirbaş U., “S355J2+N Malzemelerin Elektrocuruf Kaynak Yöntemi ile Kaynaklanabilirliği ve Mekanik Özelliklerinin İncelenmesi”, *Düzce University Journal of Science and Technology*, 8(1): 940-950, (2020).
- [22] Kou S., “Welding Metallurgy”, (Second Edition), *Department of Materials Science and Engineering University of Wisconsin*, USA, 143-393, (2003).
- [23] Çetinkaya C., Arabacı U. ve Akay A., “Yakma Alın Kaynağı İle Kaynatılmış İki Farklı Çeliğin Kaynak Kalitesine Yığma Akım Zamanının Etkisi”, *Gazi Üniv. Müh. Mim. Fak. Der.*, 21: 519-525, (2006).
- [24] Bahman A.R. and Alialhosseini E., “Change in hardness, yield strength and UTS of welded joints produced in St37 grade steel”, *Indian Journal of Science and Technology*, 1162-1164, (2010).
- [25] Kossakowski P.G., “Experimental Determination of the Void Volume Fraction for S235JR Steel at Failure in the Range of High Stress Triaxialities”, *Arch. Metall. Mater.*, 167-172, (2017).
- [26] Pineau A., Benzerga A.A., Pardoën T., “Failure of metals I: Brittle and ductile fracture”, *Acta Materialia*, 107: 424-483, (2016).
- [27] Biner İ., “Kaynaklı Numunelerin Tahribatlı Testlerinin Güvenilirliği ve Cihaz Kalibrasyonu”, *10th Welding technology national congress and fair*, Ankara, 125-129, (2015).
- [28] Çetinkaya C., “Düşük karbonlu çeliklerin tozaltı ark kaynak yöntemi ile kaynak edilebilirliği ve mekanik özelliklerinin incelenmesi”, *Gazi University Journal of Science*, 12(2): 279-293, (1999).
- [29] Safriwardy F., “The Effect of Welding Position on the Quality of SMAW Welding Electrode Joint AWS E 7018”, *Ist Workshop on Multidisciplinary and Its Applications*, Aceh, 278, (2018)
- [30] Ada H., Aksöz S., Fındık T., Çetinkaya C. & Gülsün M., “Tozaltı Kaynak Yöntemiyle Birleştirilen Petrol ve Doğalgaz Borularının Mikroyapı ve Mekanik Özelliklerinin İncelenmesi”, *Journal of Polytechnic*, 19 (3): 275-282, (2016).
- [31] Kaya Y. "S235JR ile S355JR Yapı Çeliklerinin Özlü Tel Elektrotla MAG Kaynak Yöntemiyle Birleştirilebilirliğinin Araştırılması", *Politeknik Dergisi*, 21(3): 597-602, (2018)